APPLICATION NOTE

ANP109 | Impedance Spectra of Different Capacitor Technologies

Réne Kalbitz

01. INTRODUCTION AND THEORETICAL BACKGROUND

Impedance and capacitance spectra (or scattering parameters) are common representations of frequency dependent electrical properties of capacitors. The interpretation of such spectra provides a wide range of electrochemical, physical and technical relevant information. Those need to be separated from the ever-present measurement artifacts as well as parasitic effects.

Since it is sometimes not possible to provide all data in the data sheet, the engineer may have to utilize measured spectra to choose the suitable component for its circuit design. To provide the best possible database, Würth Elektronik eiSos has implemented the online tool REDEXPERT, were spectra but also other measurements are provided.

In this note, we will recap the properties of such spectra and discuss how basic electrical characteristics can be inferred from it.

1.1 Equivalent Circuit of Capacitors

With the circuit, shown in Abbildung 1, it is possible to model frequency dependent impedance spectra of all capacitor types ranging from multilayer ceramic capacitor (MLCC) to Supercapacitors (SCs). [1][2][3][9]

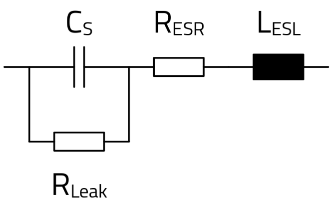

Figure 1*: Standard equivalent circuit as used for capacitors*

The formula sign C_S is the pure capacitance, which does not exist on its own as an electrical component. Any real capacitor has losses, which "slows down" the charge storing process. This phenomenon is modeled by the pure ohmic equivalent series resistance R_{ESR} (ESR). The resistance of the current collector and the leads also contribute to the ESR.

The pure lossless capacitance is defined by a differential:

$$C_S = \frac{dQ}{dV} \qquad (1)$$

with dQ as the change of number of charges at the capacitor interface and dV as the change of voltage at the capacitor.

Any alternating current in a metal conductor induces a magnetic field that opposes the current. In our model, this property is described by the equivalent series inductance L_{ESL} (ESL). Sometimes it is also referred to as parasitic inductance. C_S, R_{ESR} as well as L_{ESL} are the most important parameters, necessary to describe the majority of all spectra. In the most basic approach, they are constants and do not change with frequency, which is sufficiently accurate for electrical engineering.

The loss of charges over time, i.e. the leakage current, is described in good approximation by the pure ohmic resistance R_{Leak}. Usually R_{Leak} is magnitudes larger than R_ESR and can often be neglected, i.e $R_{Leak} \rightarrow \infty$. As we will see, its effect may only be visible in the spectra at very low frequencies below 1 Hz or so. A correct description of leakage current is, however, a physically complex issue, which may depend on further parameters such as pre-poling times and temperature. For technical measurement reasons, it is therefore common practice not to state R_{Leak} but the value of leakage current, along with its measurement conditions in the datasheet.

This equivalent circuit in Abbildung 1 also yields the possibility to model practically any

- voltage,
- environmental (e.g. temperature) or
- nonlinear frequency

dependency. In this case, all model parameters are simply replaced by suitable mathematical functions or entire circuit sections are replaced by distributed networks. [3][20][12][11][7]

1.2 The Impedance and Capacitance Spectra

In the following paragraph, we define frequently used terms and measured quantities, such as capacitance and impedance. [1] The above circuit can be expressed as frequency dependent complex impedance $\hat{Z}$, capacitance $\hat{C}$, scattering parameter (S-Paramter) $\hat{S}$, permittivity $\hat{\epsilon}$ or any other measureable complex electrical quantity. Passive components are often characterized in terms of capacitance and impedance. We will therefore lay the focus on these two quantities.

Impedance $\hat{Z}=\mathrm{Re}(\hat{Z})+i\cdot\mathrm{Im}(\hat{Z})$, is a complex quantity, with $\mathrm{Re}(\hat{Z})$ and $\mathrm{Im}(\hat{Z})$ as real and imaginary part, respectively. It is often expressed in terms of its magnitude $\hat{Z}$ and phase angle ϕ,

$$\hat{Z}=|\hat{Z}|\cdot e^{i\phi} \quad (2)$$ [2]

In a complex plane, as given in Figure 2, ϕ describes the angle between $\mathrm{Re}(\hat{Z})$ (abscissa) and the complex vector $\hat{Z}$. Physically, $|\hat{Z}|$ represents the ratio of the voltage amplitude to the current amplitude, while ϕ gives the phase difference between voltage and current at a given frequency. The phase angle ϕ is related to the loss angle with

$$\arctan\left(\frac{\mathrm{Re}(\hat{Z})}{|\mathrm{Im}(\hat{Z})|}\right)=\delta=\frac{\pi}{2}-\phi \quad (3)$$

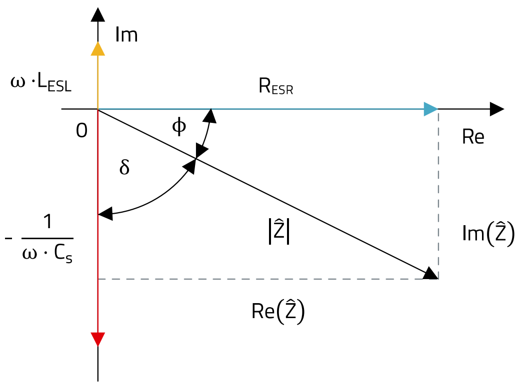

Figure 2*: Vector representation of impedance in the complex plane. R_{Leak} is neglected for the sake of simplicity.*

In electrical engineering, it is also common to use magnitude $|\hat{Z}|$ and its equivalent series resistance $R_{ESR} = \mathrm{Re}(\hat{Z})$. With the model in Figure 1 the equivalent series resistance is the real part of the impedance. In order to graphically show the relation between model and complex quantity $\hat{Z}$, all model parameters (apart from R_{Leak}) are also given in Figure 2 (Mathematical description is given in the appendix.)

The impedance may also be transferred into complex capacitance with

$$\hat{C}=\frac{1}{i\cdot 2\cdot\pi\cdot f\cdot\hat{Z}}=\mathrm{Re}(\hat{C})+i\cdot\mathrm{Im}(\hat{C}) \quad (4)$$

All these quantities, such as $\mathrm{Re}(\hat{Z})$, $\mathrm{Im}(\hat{Z})$, $|\hat{Z}|$ or δ, can be measured with impedance or network analyzers. Any electronic part (not only capacitors) can be characterized by a pair of frequency dependent quantities, such as $\mathrm{Re}(\hat{Z})$ and $\mathrm{Im}(\hat{Z})$ or $\mathrm{Re}(\hat{C})$ and $\mathrm{Im}(\hat{C})$. However, it is only due to equivalent circuits such as given in Figure 1, by which measurement results can be interpreted. The model (also referred to as standard model) provides the mathematical means to extract the electric parameters C_S, R_{ESR}, L_{ESL} and R_{Leak}.

It is not only possible to use the model for the extraction of parameters, it can also be used to calculate theoretical spectra.

By changing C_S, R_{ESR}, L_{ESL}, R_{Leak}, it is possible to describe or calculate the basic frequency behavior for all capacitors. This is exemplary demonstrated for impedance and capacitance spectra of a 4.7 µF and a 50 F capacitor, given in Figure 3 and Figure 4, respectively. In Figure 4, dashed-dotted lines designate the pure capacitive and inductive contributions. The parameters for the two examples are as follows:

- Supercapacitor (WCAP-STSC) with C_S = 50 F, R_{ESR} = 5 mΩ, L_{ESL} = 5 nH and R_{Leak} = 10 MΩ,
- Film capacitor (WCAP-FTBE) with CS = 4.7 µF, R_{ESR} = 15 mΩ, L_{ESL} = 5 nH and R_{Leak} = 10 MΩ.

The parameters were chosen such, as to fit to actual Würth Elektronik eiSos products found under the match code for film capacitors WCAP-FTBE (4.7 µF) and SCs WCAP-STSC (50 F). In these plots, C_S, R_{ESR}, L_{ESL} and R_{Leak} were assumed to be constants and independent of frequency (Table 1). This assumption is in most cases in good agreement with actual measurements. However, especially for the R_{ESR} a frequency dependence in real measurements is noticeable, as will be discussed in the following sections..

Electrical Parameter	WCAP-FTBE	WCAP-STSC
C_S	4.7 µF	50 F
R_{ESR}	5 mΩ	15 mΩ
L_{ESL}	5 nH	5 nH
R_{Leak}	10 MΩ	10 MΩ

Table 1: Electrical Parameters used for calculation of spectra.

As mentioned above, we may also think of it the other way round. With this single model, it is possible to derive the product parameters from a measured curve.

Before we look at measured graphs, it is worth the while to have a look at theoretical graphs. They have the advantage that they can be generated for any frequency range, which allows the representation of all features, such as characteristic frequencies, in one graph. [3]

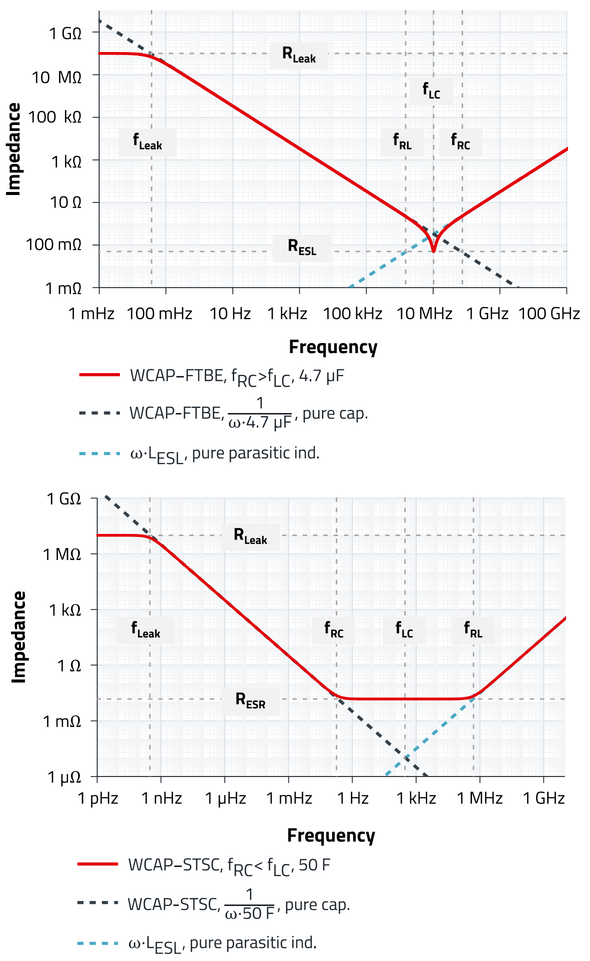

Figure 3: *Impedance spectra $|\hat{Z}|$ for WCAP- FTBE (Top) and WCAP-STSC (Bottom) as calculated from the standard model*

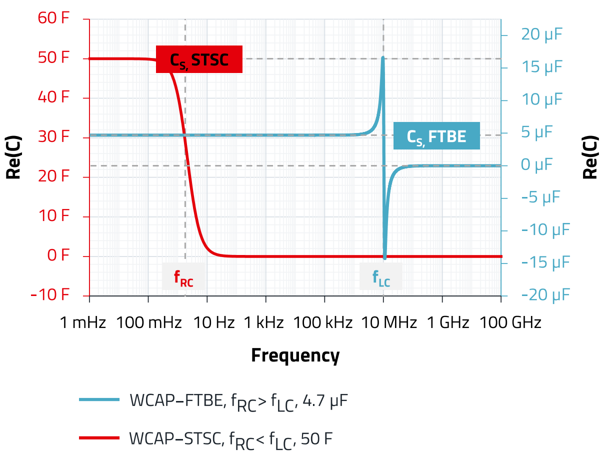

Figure 4: *Capacitance spectra Re ($\hat{C}$), as calculated from the standard model. Graph for WCAP-STSC (orange) corresponds to left hand ordinate and the graph for the WCAP-FTBE (blue) corresponds to the right hand ordinate.*

Generally, the position of the most prominent features of the spectra are described by four characteristic frequencies:

Characteristic frequency of the R_{ESR}-C unit:

$$f_{RC}=\frac{1}{2\cdot\pi\cdot R_{ESR}\cdot C_S} \tag{5}$$

Characteristic frequency of the L-C unit:

$$f_{LC}=\frac{1}{2\cdot\pi\cdot\sqrt{L_{ESL}\cdot C_S}} \tag{6}$$

Characteristic frequency of the R_{Leak}-C unit:

$$f_{Leak}=\frac{1}{2\cdot\pi\cdot R_{Leak}\cdot C_S} \tag{7}$$

Characteristic frequency of the R_{ESR}-L unit:

$$f_{RL}=\frac{R_{ESR}}{2\cdot\pi\cdot L_{ESL}} \tag{8}$$

Two main situations can be distinguished in Figure 3 and Figure 4:

- Lorentz-Oscillation: $f_{RC} > f_{LC}$ as in the case for $C_S = 4.7$ µF (blue graph) and
- Debye-Relaxation: $f_{RC}<f_{LC}$ as in the case for $C_S = 50$ F (orange graph). [4][5]

Horizontal dash-dotted lines in both graphs signify the pure capacitive and inductive part. For the imaginary part of the capacitance, please refer to Figure 17 in the appendix.

f_{RC}, the characteristic frequency of the R-C unit, is the frequency at which the capacitor can be charged and discharged. The inverse of the frequency is basically the charging time under ideal constant voltage charging. For the capacitor with $C_S = 50$ F, the ideal charging time is about $2\cdot\pi\cdot 15\ m\Omega\cdot 50\ F\approx 5$ sec Below the frequency of (5 sec)^(-1) the capacitor can utilize its nearly full capacitance (>99.9 %). Above this frequency, the capacitor is not fully charged anymore (in reference to the maximum voltage of the AC signal).

At f_{RC} the capacitance spectrum (Figure 4) of the Supercapacitor shows a shoulder. Below this frequency, the capacitance value can be inferred from the graph. Above f_{RC} the impedance spectrum, given in Figure 3 (Bottom), shows a plateau at R_{ESR}.

f_{LC}, the characteristic frequency of the L-C unit, is the frequency at which the coupling of parasitic inductance and capacitance leads to a resonant behavior (if $f_{RC} > f_{LC}$). Below this frequency the capacitor acts as capacitor, i.e. can be charged. Above this frequency the capacitor acts as inductor. The self-resonance results in a sharp minimum in the impedance spectrum (WCAP-FTBE), as given in Figure 3 (Top).

At the minimum of the impedance spectrum the R_{ESR} value can be read off.

The capacitance spectrum in Figure 4 shows a pole, which is a special type of singularity. It is actually a real physical behavior and not only a measurement artefact.

The measurement system, which consists of the capacitor and the parasitic inductance, behaves like a oscillator, i.e. resonator. [4]

At the increasing positive branch, the probing signal constructively contributes to the oscillations of the resonator. That is to say, the charge increase dQ at the interface is disproportionately high, although the magnitude of applied voltage signal dV remains the same. Since $C_S = dQ/dV$, a strong increase of the capacitance is measured. At the maximum, the system is in phase (resonance) with the probing frequency.

A further increase of the probing frequency leads to an abrupt change in sign of the capacitance (singularity). at f_{LC}.

At the negative branch, the probing signal destructively overlaps with the oscillations of the resonator. The current is actually flowing "in opposite direction" to the probing voltage.

Thus, the applied voltage signal dV leads effectively to a relative decrease of charge at the capacitor interface –dQ, which results in a negative capacitance.

f_{Leak} is the characteristic frequency of the R_{Leak}-C unit. Below this frequency the capacitor acts like a resistor with resistance R_{Leak}. That is to say, at very low frequencies, the leakage discharge is larger than the AC charging current. Usually this effect is rarely visible in the spectra. It requires either measurements to frequencies below 1 Hz or a rather low R_{Leak}.

f_{RL}, the characteristic frequency of the R_{ESR}-L unit, is the frequency above which the capacitor acts like an inductor with inductance L_{ESL}. In cases where $f_{RC} < f_{LC}$, it signifies the onset of the increase in impedance at high frequencies. Above this frequency, it is exceedingly difficult to extract R_{ESR} values from measured impedance spectra.

02. MEASURED IMPEDANCE SPECTRA AND CAPACITANCE SPECTRA

The following sections will discuss spectra on different capacitor types, exemplarly chosen from the Würth Elektronik eiSos portfolio. The standard model, depicted in Figure 1, uses an frequency independent ohmic resistance R_{ESR}. However, physical processes as well as measurement artifacts may lead to deviations from the idealized ohmic behavior, as will be seen in the below section [6][7]

2.1 Supercapacitors WCAP-STSC

The below presented spectra were measured with the impedance analyzer Alpha-AK, POT/GAL from Novocontrol in a four-terminal Kelvin configuration. The four-terminal Kelvin configuration has the advantage of enabling a high phase angle resolution of about 0.001 °, since the voltage measurement probes are independent from the current supply leads.

The measured impedance spectrum of a SC with 50 F in Figure 5 shows the same features as the corresponding theoretical spectrum in Figure 3.

In this case ($f_{RC} < f_{LC}$), f_{RC} is below 1 Hz and thus several magnitudes smaller than f_{LC}. As a result, the spectrum shows a flat bottom region from which R_{ESR} can be inferred. The increase of R_{ESR} towards lower frequencies is more clearly visible in the spectrum of $Re(\hat{Z})=R_{ESR}$ in Figure 6.

This frequency dependence is not a measurement artefact, however, attributed to real physical phenomena:

- distributed network of porous electrodes and
- the ionic charge transport in the electrolyte of the EDLC. [8][9][10][11][12][13]

A physical interpretation of the spectra is: The slower the SC is charged, the more pores can be infiltrated by charges, which leads to the increase of capacitance. Due to the viscous solvent, the ions require more time to insert the smaller pores, which in turn leads to an increase of R_{ESR} toward low frequencies.

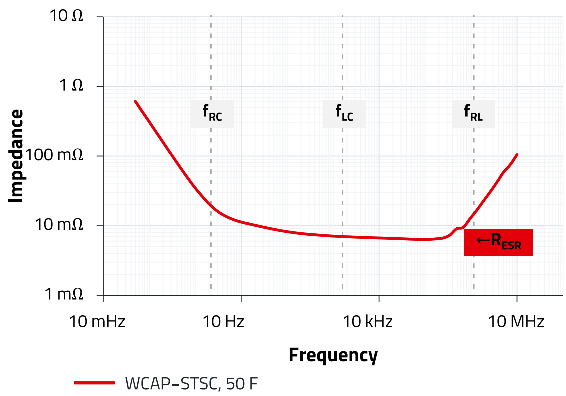

Figure 5: *Measured impedance spectrum* $|\hat{Z}|$ *d of 50 F Supercapacitor, WCAP-STSC*

The values of $Re(\hat{Z}) = R_{ESR}$ below f_{RC} and above f_{LC} become unreliable, since the spectra become dominated by the capacitive and parasitic inductive behavior.

The shoulder at f_{Leak} is not visible, since it is practically difficult to measure toward such low frequencies. (Also for other capacitor technologies, it is not common practice to measure at such low frequencies. The shoulder at f_{Leak}. is usually not depicted in impedance spectra.)

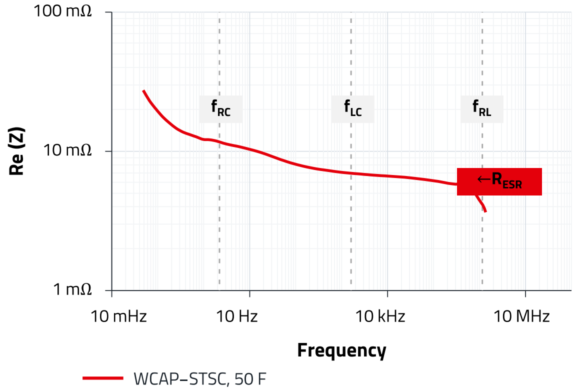

Figure 6*: Measured spectrum of the real part of the impedance (Re($\hat{Z}$)=R_{ESR}) of 50 F Supercapacitor, WCAP-STSC..*

The capacitance spectrum in Figure 7 shows the typical shoulder situated at the characteristic frequency of the R_{ESR}-C unit f_{RC}. The height of the shoulder is at about 51 F (0.01 Hz) with a slight increase toward lower frequencies. This increase is especially pronounced in electrolytic capacitors such as Supercaps. It is, as already mentioned above, mainly caused by the charge storing at porous interfaces as well as pseudo capacitive processes. Mathematically, it can be well described by a set of distributed R-C networks.[3]

The characteristic frequency is, as shown above, governed by the term R_{ESR} C_S. Due to the relatively high capacities, the characteristic frequencies has to shift to frequencies around or even below 1 Hz. The indicated frequency f_{RC} Figure 7 is about 0.21 Hz. The inverse of f_{RC} can be interpreted as lower limit for the constant voltage charging time, which in this case is:

$$\frac{1}{f_{RC}} = \frac{1}{0.21\ \text{Hz}} \approx 5\ \text{s}. \qquad (9)$$

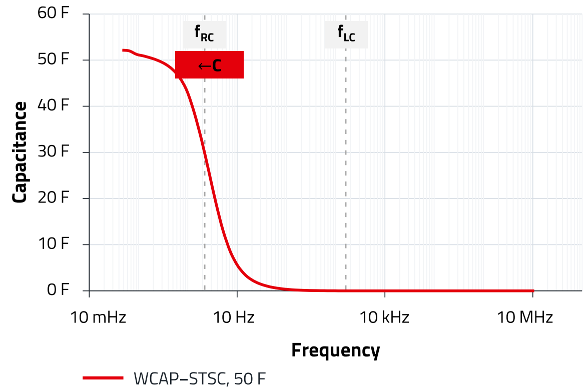

Figure 7*: Measured capacitance spectrum of 50 F Supercapacitor, WCAP-STSC*

The following characteristic values can be extracted from the measured spectra above:

- C_S (0.01 Hz)=51 F
- R_{ESR} (f_{RC}=0.2 Hz) = 0.012 Ω
- R_{ESR} (f_{LC}=160 Hz) = 0.007 Ω

2.2 Aluminum Electrolytic Capacitors, WCAP-AIG8

The following spectra were measured with the impedance analyzer Alpha-AK, POT/GAL from Novocontrol in a four-terminal Kelvin configuration.

In principle, the charge storing mechanism of the aluminum electrolytic capacitor (E-Cap) is comparable to the one of the SC. The energy is stored by electrolytic charges at a porous interface. However, the E-Cap utilizes a thin porous aluminum oxide layer as a dielectric. The porosity of this layer again leads to large effective surfaces and relatively large capacitance. It is due to the large capacitance that for this type of capacitor f_{RC} is often (not always!) still lower than f_{LC}, as indicated in the measured impedance spectrum of a 270 µF capacitor in Figure 8. Compared to the SC, f_{LC} has shifted towards higher frequencies. The capacitive contribution is more pronounced and thus appears also further shifted to higher frequencies. The contribution of the parasitic inductance is about the same. Hence, the flat bottom region is much smaller than for the SC.

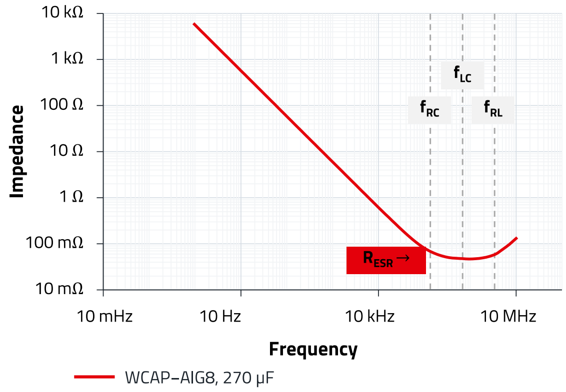

Figure 8*: Measured impedance spectrum $|\hat{Z}|$ of 270 µF aluminum electrolytic capacitor.*

In general, all features of the spectra in Figure 9 and Figure 10 appear shifted to higher frequencies. The interpretation of the capacitance spectrum in Figure 9, with its characteristic shoulder, is similar to the one for the SC.

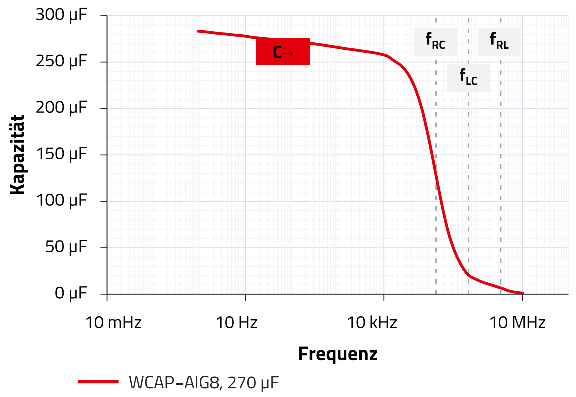

Figure 9*: Measured capacitance spectrum of 270 µF aluminum electrolytic capacitor.*

The equivalent series resistance $Re(\hat{Z})=R_{ESR}$, given in Figure 10, also shows the increase toward low frequencies. However, below 1 kHz or so the spectrum shows a strong increase toward lower frequencies. This strong increase is however, probably not due to any real physical effect, it is a measurement artefact. It is a common effect that always happens, if the loss angle is very close to zero. In this region, the equipment is not able to clearly separate the real and imaginary part from each other, which results in an overestimated output of the real part.

Hence, the correct interpretation of the spectra at low loss angles, which corresponds to low or high frequencies with respect to f_{LC}, is usually difficult, since the loss angle resolution of the most LCR meters is not smaller than 0.1 degree or so. However, that also means that generally the values around or at f_{LC} are most trustworthy.

At the end, a correct interpretation of any impedance spectra is only possible with the experimental details of the measurement.

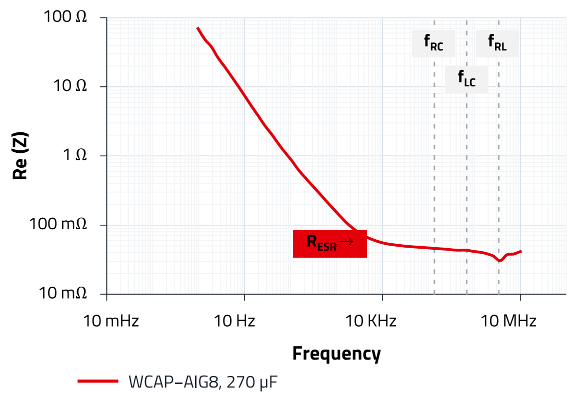

Figure 10*: Measured spectrum of the real part of the impedance ($Re(\hat{Z}) = R_{ESR}$) of 270 µF aluminum electrolytic capacitor.*

The following characteristic values can be extracted from the measured spectra above. The dissipation factor $DF = R_{ESR}/X_c = 2\pi f C_S R_{ESR}$ is stated to improve comparability with data sheets and other documentations. The results for frequencies $\ll f_{LC}$ are given for the sake of completeness. They may contain a large error as is explained in the Appendix and elsewhere. [14][6][15][16]

- C_S (120 Hz) = 265 µF
- R_{ESR} (120 Hz) = 0.14 Ω Ω
- R_{ESR} (f_{LC} = 68.5 kHz) = 0.04 Ω
- DF (120 Hz) = $R_{ESR}/X_c = 2\pi f C_S R_{ESR}$ = 2.8 %
- DF (f_{LC} = 68.5 kHz) = $2\pi f C_S R_{ESR}$ = 0.8 %.

  (Capacitive Reactance: $X_c = 1/(2\pi f C_s)$)

2.3 Film Capacitors, WCAP-FTBE

The below spectra were measured with Agilent E5061B Network Analyzer in a shunt through configuration. [15]

The measured impedance spectrum of a 470 nF Film capacitor, in Figure 11, shows in principle the same features as the calculated spectra, given in Figure 3 (Top). Due to the low capacitance $f_{RC} > f_{LC}$, as indicated by the dashed lines, which results in a graph with a sharp minimum at f_{LC} = 1.94 MHz. The resistance value at the minimum is roughly the R_{ESR} at f_{LC}, which in this case is about 0.04 Ω.

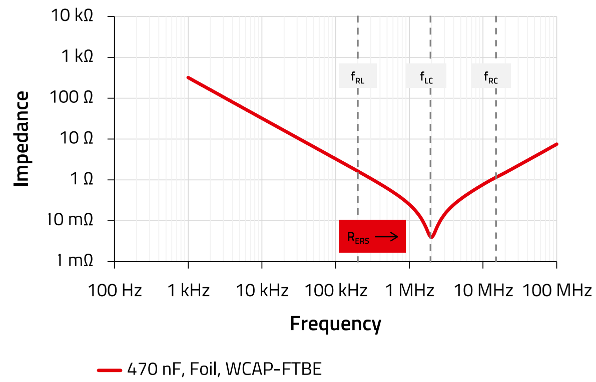

Figure 11*: Measured impedance spectrum $|\hat{Z}|$ of 470 nF film capacitor.*

The measured spectrum of the equivalent series resistance $Re(\hat{Z})=R_{ESR}$, given in Figure 12, shows a bathtub-like shape with a minimum around f_{LC}. The increase at high and low frequencies is very likely not the actual physically correct ESR behavior of the capacitor, but a measurement artifact from the low capacitance (high impedance) and the parasitic inductance.

The separation of a small real part from a large imaginary part is technically difficult. At the end the accuracy and the resolution of measurable loss angle, i.e phase angle, determines the accuracy of the measured impedance. Accuracy plots for the used equipment (Figure 22, Figure 24) and an error calculation for this measurement is given in the

Appendix. At these demanding conditions, analyzers often overestimate Re($\hat{Z}$). [14][6][15]

The network analyzer has no separate current and voltage connections, which usually leads to a lower phase accuracy than for four-terminal Kelvin configurations. Hence, it is a common phenomenon that ESR values, if measured in such a configuration, are overestimated. For the sake of prudency, it is best to consider those values as conservative estimates.

Hence, it is practically difficult to say to what extend the measured Re($\hat{Z}$) in Figure 12 is correct. Certainly around f_{LC} the results of approximately 0.04 Ω are most trustworthy and can be considered as an conservative estimate.

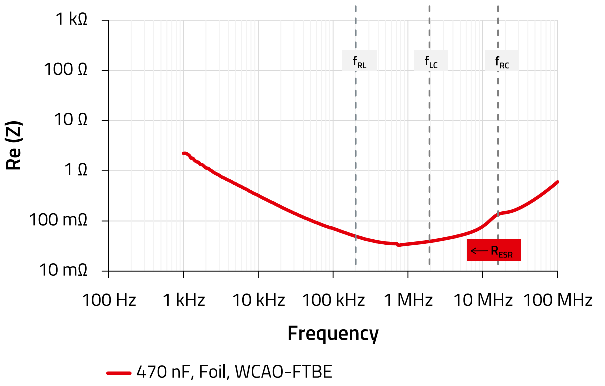

Figure 12*: easured spectrum of the real part of the impedance (Re($\hat{Z}$)=R_{ESR}) of a 470 nF film capacitor*

The measured capacitance spectrum in Figure 13 shows the overall features of the calculated spectrum, given Figure 4. It has a plateau region at low frequencies and a singularity, positioned at f_{LC}. The measured capacitance, as read of from the plateau region, is about 495 nF. The measured capacitance with its hyperbolic behavior is physically correct and not some sort of measurement artefact (see section 1.2).

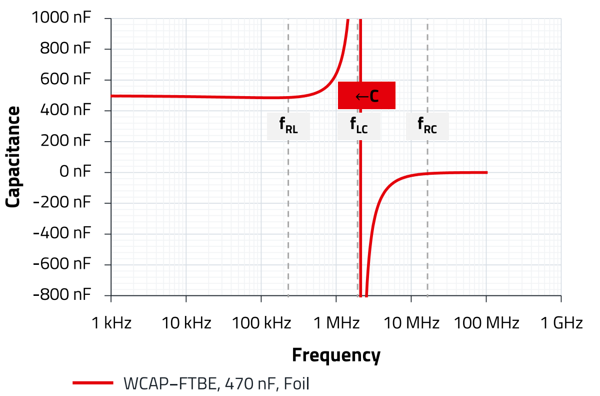

Figure 13*: Measured capacitance spectrum of a 470 nF film capacitor.*

The parasitic inductance may change as function of the length of circuit path or temperature. As a consequence, also the position of f_{LC} may change accordingly. It is therefore in practice important to operate the application not in the vicinity of f_{LC}.

The following characteristic values can be extracted from the measured spectra above. The dissipation factor $DF = R_{ESR}/X_c = 2\pi f C_S R_{ESR}$ is calculated to improve comparability with data sheets and other documentations. The results for frequencies $\ll f_{LC}$ are given for the sake of completeness. They may contain a large error as explained in the Appendix and elsewhere.. [14][6][15][16]

- C_S (1 kHz) = 495 nF
- R_{ESR} (1 kHz) = 2.2 Ω
- R_{ESR} (f_{LC}=1.94 MHz) = 0.04 Ω
- DF(1 kHz) = $2\pi f C_S R_{ESR}$ = 0.68 %
- DF(f_{LC}=1.94 MHz) = $2\pi f C_S R_{ESR}$ = 24 %.

2.4 Multilayer Ceramic Chip Capacitor, WCAP-CSGP

The following spectra were measured with Agilent E5061B Network Analyzer in a shunt through configuration.

The impedance spectrum, given in Figure 14, is qualitatively the same as for the film capacitor in section 2.3. Due to the lower rated capacitance of 22 nF the impedance spectrum is shifted to higher frequencies with f_{LC} = 45.8 MHz. As in the last chapter $f_{RC}>f_{LC}$, which leads to a sharp minimum at f_{LC}

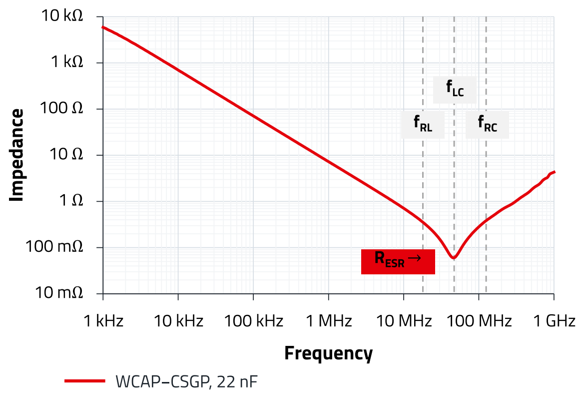

Figure 14*: Measured impedance spectrum $|\hat{Z}|$ of 22 nF MLCC.*

The ESR, as inferred from the minimum at f_{LC}, is about 0.06 Ω, which for the same reasons as discussed in section 2.3, could be considered as conservative estimate. The actual ESR might be even lower.

The capacitance spectrum in Figure 15 shows, as discussed above, the typical resonant behavior. From its constant plateau region we may read a capacitance of about 23 nF..

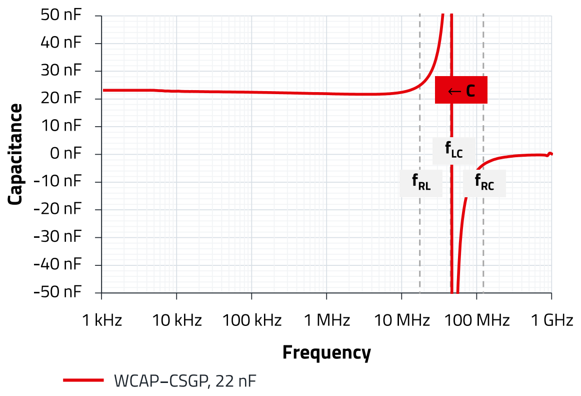

Figure 15*: Measured capacitance spectrum of 22 nF MLCC.*

Figure 16 shows the ESR spectrum with a shallow bathtub like shape. As discussed in the last chapter, the increase toward low and high frequencies is probably the result of incorrect separation of real and imaginary part of the impedance by the measurement equipment, i.e. small loss angle δ

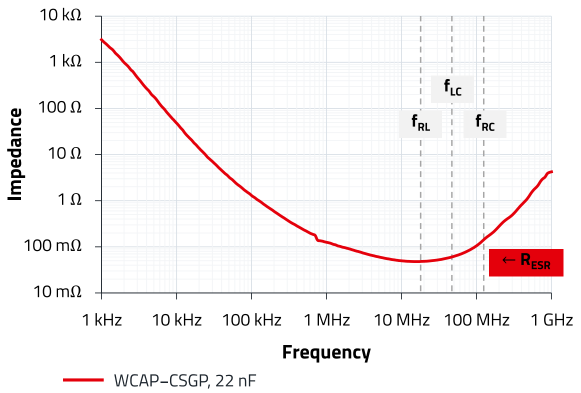

Figure 16*: Measured spectrum of the real part of the impedance ($Re(\hat{Z})=R_{ESR}$) of 22 nF MLCC*

The increase toward lower frequencies could be partially explained with the increase in dielectric loss due to ionic polarization of larger domain structures or charge hopping induced conductivity. However, the actual value of about $Re(\hat{Z})$ = 3000 Ω at 1 kHz clearly suggests, that the increase is largely attributed to an insufficient resolution of the loss angle. As mentioned before, it is technically difficult to separate the real part from a relatively large imaginary part, i.e. small loss angle (see Appendix, Figure 23).

The increase toward higher frequencies could be due to the skin effect. The geometrical factor of the electrodes of an MLCC makes a scientifically sound analysis of this effect difficult. Usually studies of skin effect are conducted on cylindrical geometries. Those results cannot be quantitatively used for measurements of MLCCs.. [17][18][19]

Due to the resolution limits of the loss angle, the $Re(\hat{Z}) = R_{ESR}$ spectra have often a minimum around f_{LC} and strongly increasing slopes toward low and high frequencies. This measurement effect will superimpose any potential skin-effect (see Figure 25) [17]

To cut a long story short, ESR spectra of LCR resonators are most trustworthy in the region around f_{LC}. Beyond that, they require, not always but often, further technical knowledge for interpretation.

The following characteristic values can be extracted from the measured spectra above. The dissipation factor $DF = R_{ESR}/X_c = 2\pi f C_S R_{ESR}$ is given to improve comparability with data sheets and other documentations. The results for frequencies $\ll f_{LC}$ are given for the sake of completeness. They may contain a large error as is explained in the Appendix and elsewhere. [14][6][15][16]

- C_S (1 kHz) = 23 nF
- R_{ESR} (f_{LC} = 46 MHz) = 0.06 Ω
- $DF(f_{LC} = 46\text{ MHz}) = 2\pi f C_S R_{ESR}$ = 38 %

03. CONCLUSION

The standard model, given in Figure 1, is a suitable means to interpret the technically important features of all commercially relevant capacitors. In most cases, it is even sufficient to use an even simpler model, which neglects R_{Leak}. It was furthermore demonstrated how the model parameters, such as C_S and R_{ESR}, can be extracted from measured spectra.

The deviations from that model as well as aspects of the measurement accuracy have been exemplarily discussed on measured spectra. Especially the separation of real and imaginary part at small loss angles is defective. In the self-resonant case, the R_{ESR} spectra can only be correctly measured around f_{LC}. Due to this reason the physical phenomena, such as skin effect, are very likely superimposed by a large error and cannot be studied in the measured R_{ESR} spectra.

A Appendix

A.1 Graphs and Figures

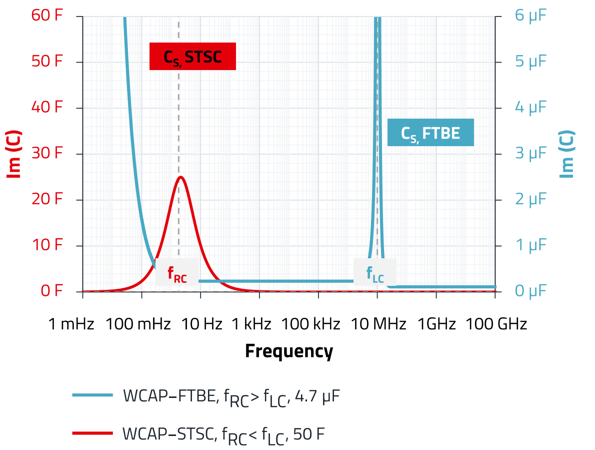

Figure 17*: Capacitance spectrum Im($\hat{C}$) as calculated from the standard model. Corresponds to spectrum Re($\hat{C}$) in Figure 4. Gray lines indicate Re($\hat{C}$).*

Interpretation of Im($\hat{C}$) (Figure 17) for R-C unit: Im($\hat{C}$) describes the dissipation of energy in a capacitive system, associated to the movement of charges. This dielectric relaxation, i.e. absorption band, is caused by the reorientation of permanent molecular dipoles, induced by the applied alternating electric field.

Im($\hat{C}$) is mathematically related to the Re($\hat{C}$) by the Kramers-Kronig relation. In case of a Debye relaxation, Im($\hat{C}$) can be conveniently used to read off f_{RC}. The height of peak of Im($\hat{C}$) at f_{RC} is for the Debye relaxation $C_S/2$.

An example of calculation for a Lorentz oscillation ($f_{RC} > f_{LC}$) is given in Figure 18. The parameters for the plot are such as to show all details of the curve progression. The graph does not necessarily correspond to a specific capacitor product.

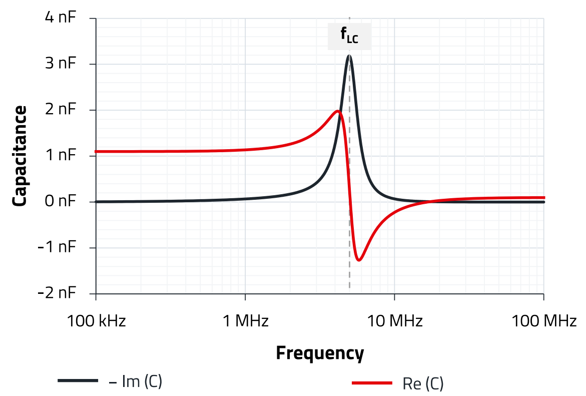

Figure 18*: Example of calculation for a Lorentz relaxation ($f_{RC} > f_{LC}$), Parameters are such as to see all details.*

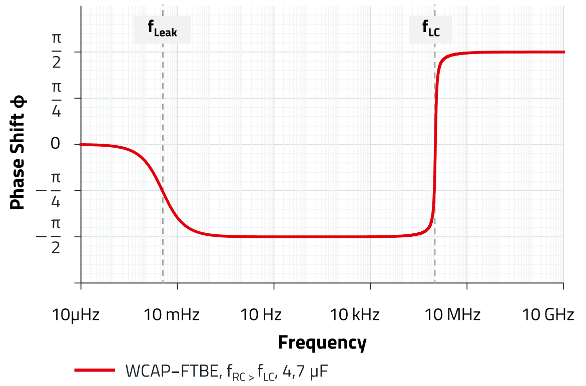

Figure 19*: Phase shift angle ϕ(f) for WCAP-FTBE as calculated from the standard model. Corresponds to impedance spectra in Figure 3. Polarization contributions at higher frequencies, such as electronic polarizations, are neglected, i.e. C(f→∞)=0*

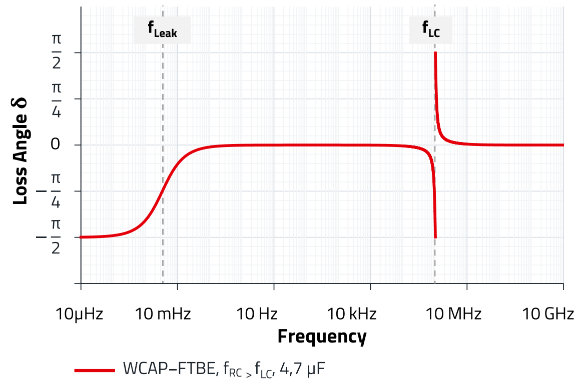

Figure 20*: Loss angle δ (f) for WCAP-FTBE as calculated from the standard model. Corresponds to impedance spectra in Figure 3. Polarization contributions at higher frequencies, such as electronic polarizations, are neglected, i.e. C(f→∞)=0.*

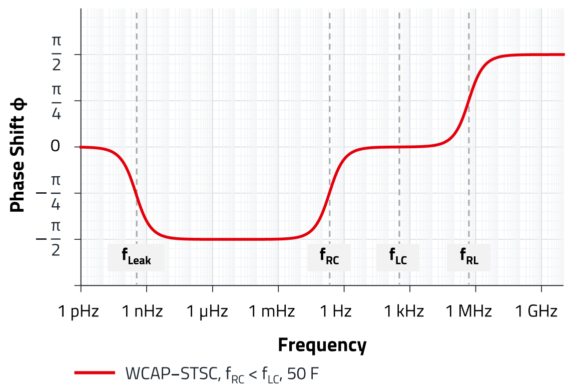

Figure 21: *P Phase shift angle ϕ(f) for WCAP-STSC as calculated from the standard model. Corresponds to impedance spectra in Figure 3. Polarization contributions at higher frequencies, such as electronic polarizations, are neglected, i.e. C(f→∞)=0.*

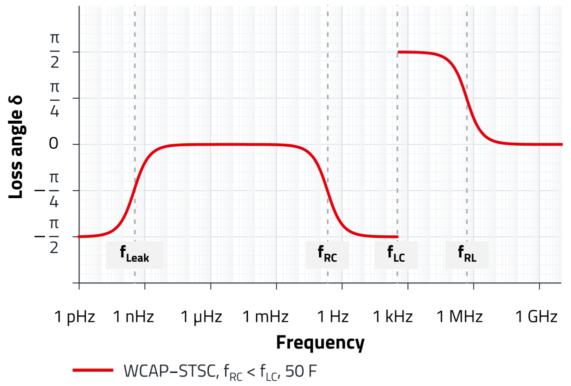

Figure 22*: Loss angle δ (f) for WCAP-STSC as calculated from the standard model. Corresponds to impedance spectra in Figure 3 Polarization contributions at higher frequencies, such as electronic polarizations, are neglected, i.e. C(f→∞)=0.*

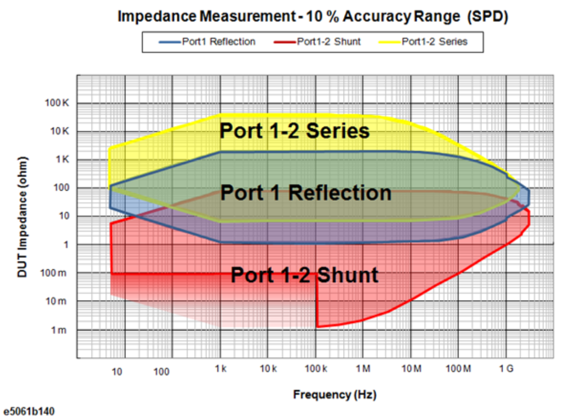

Figure 23*: Accuracy plot for E5061B ENA Vector Network Analyzer from Keysight. Conditions for 10 % measurement accuracy range (Source: externally*[15]*)*

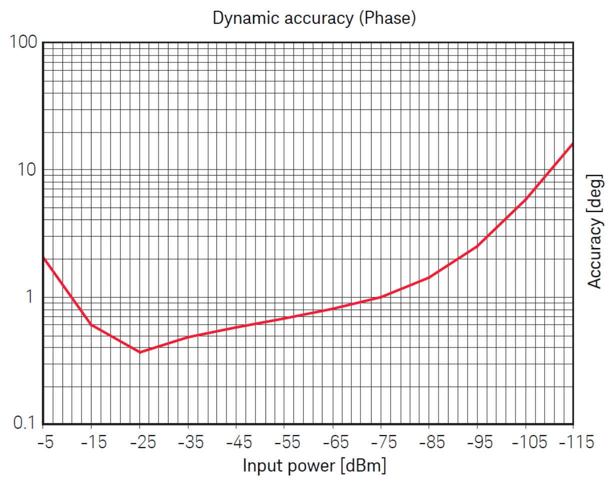

Figure 24*: Phase accuracy for E5061B ENA Vector Network Analyzer from Keysight. (Source: externally*[15][16]*)*

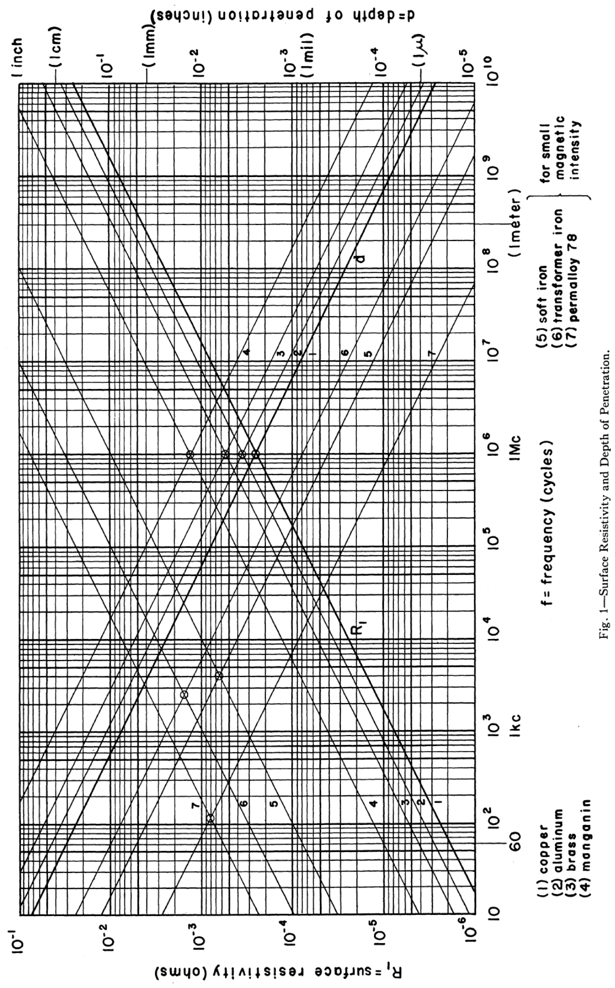

Figure 25*: Surface resistivity and depth of penetration for different materials at room temperature. (Source: externally*[17]*)*

A.2 Formulas and Notes

Mathematical description of the equivalent circuit in section 1.1 (temporal frequency: f, angular frequency: $\omega=2\cdot\pi\cdot f$)

$$\hat{Z}(\omega)=R_{ESR}+i\cdot\omega L_{ESL}+\frac{R_{Leak}(i\omega C_S)^{-1}}{R_{Leak}+(i\omega C_S)^{-1}} \quad \text{(A1)}$$

$$\hat{Z}(\omega)=\mathrm{Re}(\hat{Z})+i\cdot\mathrm{Im}(\hat{Z}) \quad \text{(A2)}$$

$$\mathrm{Re}(\hat{Z})=\frac{\omega^2 R_{ESR}R_{Leak}^2C_S^2+R_{ESR}+R_{Leak}}{\omega^2 R_{Leak}^2C_S^2+1} \quad \text{(A3)}$$

$$\mathrm{Im}(\hat{Z})=\frac{\omega(\omega^2 R_{Leak}^2L_{ESL}C_S^2-R_{Leak}^2C_S+L_{ESL})}{\omega^2 R_{Leak}^2C_S^2+1} \quad \text{(A4)}$$

$$\hat{Z}(\omega)=\frac{(i\omega)^2R_{Leak}L_{ESL}C_S+i\omega(R_{ESR}R_{Leak}C_S+L_{ESL})+R_{ESR}+R_{Leak}}{i\omega R_{Leak}C_S+1} \quad \text{(A5)}$$

In electrical engineering $\mathrm{Re}(\hat{Z})$ and $\mathrm{Im}(\hat{Z})$ are referred to as equivalent series resistance and equivalent series reactance, respectively. The dissipation factor DF is calculated with:

$$DF=\frac{\mathrm{Re}(\hat{Z})}{\mathrm{Im}(\hat{Z})} \quad \text{(A6)}$$

$$DF=\frac{\omega^2 R_{ESR}R_{Leak}^2C_S^2+R_{ESR}+R_{Leak}}{\omega(\omega^2 R_{Leak}^2L_{ESL}C_S^2-R_{Leak}^2C_S+L_{ESL})} \quad \text{(A7)}$$

With the relation $\hat{Z}=1/i\omega\hat{C}$ capacitance is calculated under the simplification that $R_{Leak}\rightarrow\infty$ und $L_{ESL}\rightarrow 0$:

$$\hat{C}(\omega)=\frac{C_S}{1+(\omega\, R_{ESR}\, C_S)^2}-i\cdot\frac{\omega C_S^2R_{ESR}}{1+(\omega R_{ESR}\, C_S)^2} \quad \text{(A8)}$$

Characteristic frequency of the R_{ESR}-C unit: Solution of equation $\mathrm{Im}[\hat{C}(f_{RC})]=C_S\frac{1}{2}$ is

$$f_{RC}=\frac{1}{2\cdot\pi\cdot R_{ESR}\cdot C_S}$$

Characteristic frequency of the L-C unit:

Solution of $\mathrm{Im}(\hat{Z}(\omega_{LC}))=0$ yields

$$\omega_{LC}=2\pi f_{LC}=\frac{1}{\sqrt{L_{ESL}\cdot C_S}}$$

Characteristic frequency of the R_{Leak}-C unit ($R_{Leak}\rightarrow\infty$):

A pole of equation (A5) is a zero of $I\omega R_{Leak}\, C_S+1$. The solution of $i(2\pi f_{Leak})R_{Leak}\, C_S+1=0$ yields

$$f_{Leak}=\frac{i}{2\cdot\pi\cdot R_{Leak}\cdot C_S}$$

For the sake of simplicity we keep the formula sign for the absolute value:

$$f_{Leak}=\frac{i}{2\cdot\pi\cdot R_{Leak}\cdot C_S}$$

Characteristic frequency of the R_{ESR}-L unit ($R_{Leak}\rightarrow\infty$):

Solution of $0=R_{ESR}-2\pi f_{RL}L_{ESL}$ for f_{RL} yields

$$f_{RL}=\frac{R_{ESR}}{2\cdot\pi\cdot L_{ESL}}$$

Effect of limited loss angle resolution:

Since the analyzer cannot measure loss angles below its resolution limit, DF will assume its minimum and remain constant for high and low frequencies (with respect to f_{LC}). Consequently, in those high and low frequency regimes the ESR will become proportional to the reactance, with DF as proportionality factor. Therefore, measured ESR spectra will often show a bathtub-like shape, where the position of the minimum of the ESR spectra coincides with the minimum of the impedance spectra.

To access the accuracy of the measured ESR, it is always necessary to consider the phase angle resolution. If the measured loss angle or DF is at the resolution limit of the analyzer, it is difficult to retrieve correct ESR spectra.

Example of calculation of loss angle measurement error with loss angle resolution limit δ_Δ:

The relative error associated to the $\tan\delta$ is calculated with:

$$\Delta=\frac{\tan(\delta+\delta_\Delta)-\tan\delta}{\tan\delta}\cdot 100\%$$

The results for the measured frequencies f_e in Table 2 are calculated on the basis of spectra, given in Figure 12. They exemplify the error Δ associated to the measurement of above film capacitors (WCAP-FTBE).

Parameter	Value	Value	Value
f_e in kHz	450	10	1
$\mathrm{Im}(\hat{Z})$ in Ω C_s=4.7 nF	0.75	33.86	338.63
$\mathrm{Re}(\hat{Z})$ at f_e in Ω	0.039	0.31	2.23
δ_Δ in ° (Figure 24)	0.30	0.30	0.30
tan δ	0.052	0.009	0.007
δ in °	2.967	0.525	0.377
Δ in %	10.1	57.2	79.5

Table 2: Values for exemplary error calculation

A.3 References

[1] Editors: E. Barsoukov, J. R. Macdonald, Impedance Spectroscopy: Theory, Experiment, and Applications, Third Edition, John Wiley & Sons (2018)

[2] Luis Moura and Izzat Darwazeh, Introduction to Linear Circuit Analysis and Modelling: From DC to RF, Newnes an imprint of Elsevier (2005)

[3] B. E. Conway, Electrochemical Supercapacitors - Scientific Fundamentals and Technological Applications, Kluwer Academic Publishers, Springer, Boston (1999)

[4] A. F. J. Levi, Essential Classical Mechanics for Device Physics, Morgan & Claypool Publishers (2016)

[5] R. M. Hill and L. A. Dissado, Debye and non-Debye relaxation, Journal of Physics C: Solid State Physics, 18(19):3829-3836 (1985)

[6] D Edwards, J.-H Hwang, S.J Ford, T.O Mason, Experimental limitations in impedance spectroscopy: Part V. Apparatus contributions and corrections, Solid State Ionics, 99(1,2):85-93 (1997)

[7] Jong-Sook Lee et al., Impedance Spectroscopy Models for X5R Multilayer Ceramic Capacitors, Journal of the Korean Ceramic Society, 49(5):475-483 (2012)

[8] R. Kötz et al., Temperature behavior and impedance fundamentals of supercapacitors, Journal of Power Sources, 154:550–555 (2006)

[9] M. Schönleber, E. Ivers-Tiffée, Approximability of impedance spectra by RC elements and implications for impedance analysis, Electrochemistry Communications, 58:15-19 (2015)

[10] Bing-Ang Mei et al., Physical Interpretations of Nyquist Plots for EDLC Electrodes and Devices, The Journal of Physical Chemistry C, 122(1): 194-206 (2018)

[11] M.R. Hasyim, D. Ma and R. Rajagopalan and C. Randall, Prediction of Charge-Discharge and Impedance Characteristics of Electric Double-Layer Capacitors Using Porous Electrode Theory, The Electrochemical Society, 164(13): A2899-A2913 (2017)

[12] V. Srinivasan and J. W. Weidner, Mathematical Modeling of Electrochemical Capacitors, Journal of The Electrochemical Society, 146: 1650-1658 (1999)

[13] M. Itagaki, Electrochemical Impedance and Complex Capacitance to Interpret Electrochemical Capacitor, Electrochemistry, 75(8):649-655 (2007)

[14] T. Stolzke et al., Comprehensive accuracy examination of electrical power loss measurements of inductive components for frequencies up to 1 MHz, Journal of Magnetism and Magnetic Materials, 497: 166022 (2020)

[15] Online Manual, E5061B Network Analyzer, Keysight, URL: http://ena.support.keysight.com/e5061b/manuals/webhelp/eng/?nid=-32496.1150148.00&cc=CA&lc=eng&id=1790874

[16] Data Sheet, E5061B Network Analyzer, Keysight URL: http://ena.support.keysight.com/e5061b/manuals/webhelp/eng/product_information/specifications.htm

[17] H.A. Wheeler, Formulas for the Skin Effect, Proceedings of the IRE, 30(9):412-424 (1942)

[18] A. E. Kennelly, F. A. Laws and P. H. Pierce, Experimental Researches on Skin Effect in Conductors, in Transactions of the American Institute of Electrical Engineers, 34(2):1953-2021 (1915)

[19] G. Schröder J. Kaumanns, R. Plath, Advanced measurement of AC resistance on skin-effect reduced large conductor power cables ,8th International Conference on Insulated Power Cables, Versailles – France (2011)

[20] E. Ivers-Tiffée and Aweber, Evaluation of electrochemical impedance spectra by the distribution of relaxation times, Journal of the Ceramic Society of Japan, 125(4):193-201 (2017)

IMPORTANT NOTICE

USEFUL LINKS

Application Notes
www.we-online.com/appnotes

REDEXPERT Design Plattform
www.we-online.com/redexpert

Toolbox
www.we-online.com/toolbox

Product Catalog
www.we-online.com/products

CONTACT INFORMATION

appnotes@we-online.com
Tel. +49 7942 945 - 0

Würth Elektronik eiSos GmbH & Co. KG
Max-Eyth-Str. 1 · 74638 Waldenburg
Germany
www.we-online.com